

# Determination of Monomer Reactivity Ratios Using *In situ* FTIR Spectroscopy for Maleic Anhydride/Norbornene-Free-Radical Copolymerization

Anthony J. Pasquale, Timothy E. Long

Department of Chemistry and the Center for Adhesive and Sealant Science, Virginia Polytechnic Institute and State University, Blacksburg, Virginia 24061-0212

Received 28 April 2003; accepted 1 December 2003

**ABSTRACT:** Monomer reactivity ratios for maleic anhydride (MAH) and norbornene (Nb) free-radical copolymerizations were estimated by using a linear graphical method, which is based upon the terminal model developed by Mayo and Lewis. Reactions were performed by using optimized reaction conditions that were previously determined. MAH/Nb copolymerizations (3 mol % AIBN initiator, 60% solids in THF, 65°C, 24 h). Copolymerization data were collected via *in situ* FTIR to low degrees of conversion (~10%) for copolymerizations of MAH and Nb. The following five different MAH/Nb comonomer feed molar ratios were analyzed: 40/60, 45/55, 50/50, 55/45, and 60/40. Conver-

sion data that were measured with *in situ* FTIR were employed in the rearranged copolymer composition equation to estimate MAH and Nb reactivity ratios. Both of the reactivity ratios were determined to be near 0 ( $r_{\text{MAH}} = 0.02$ ,  $r_{\text{Nb}} = 0.01$ ), which was indicative of an alternating copolymerization mechanism. The highest observed rate constant for copolymerization was obtained at an equal molar concentration of monomers. © 2004 Wiley Periodicals, Inc. *J Appl Polym Sci* 92: 3240–3246, 2004

**Key words:** radical polymerization; alternating; reactivity ratios; FTIR; photoresists

## INTRODUCTION

The most simple and quantitative statistical treatment for the determination of copolymerization behavior, which is generally referred to as the terminal model, was first hypothesized by Dostal<sup>1</sup> in 1936 and later elucidated by others.<sup>2</sup> The terminal model is based upon the assumption that the chemical reactivity of a propagating polymer chain is independent of the size or composition of the chain and is only influenced by the terminal propagating repeat unit. Although the terminal model is dependent on several assumptions and may not be the most accurate model to describe a copolymer process, it is relatively simple to apply and provides a facile starting point when evaluating copolymerizations of various monomer pairs. When two monomers,  $M_1$  and  $M_2$ , are copolymerized by free-radical methods, four reactions are feasible according to the terminal model shown in Figure 1, where  $k_{11}$  is

the rate constant for the addition of a propagating chain ending in  $M_1$  adding to monomer  $M_1$ ,  $k_{12}$  is the rate constant for the addition of a propagating chain ending in  $M_1$  adding to monomer  $M_2$ , and so on. The rate constants can then be expressed in terms of the monomer reactivity ratios,  $r_1$  and  $r_2$ , where  $r_1 = k_{11}/k_{12}$  and  $r_2 = k_{22}/k_{21}$ . Monomer reactivity ratios may be either experimentally<sup>3</sup> determined or estimated<sup>4</sup> and are generally independent of free-radical initiator and solvent with only slight temperature dependence. The different types of copolymerization behavior are subsequently described on the basis of the values of the monomer reactivity ratios. Random copolymerization results when  $r_1 = r_2 = 1$  due to the equal reactivity of the monomers toward both types of propagating chain ends and the resulting copolymer composition will directly reflect the comonomer feed. When  $r_1 r_2 = 1$ , the two different types of propagating chain ends both add preferentially to one of the monomers, which is described as ideal copolymerization. The case when  $r_1$  and  $r_2$  are much greater than 1 results in a tendency to form blocks of both monomers and is appropriately termed block copolymerization. Alternating copolymerization, which describes the situation when  $r_1 = r_2 = 0$ , is an example of chain copolymerization where each of the monomers adds preferentially to the other, which results in an alternating monomer sequence distribution along the backbone.<sup>5</sup> Monomers that are

Correspondence to: T. E. Long (telong@vt.edu).

Contract grant sponsor: Jeffress Memorial Trust.

Contract grant sponsor: Virginia Tech Department of Chemistr.

Contract grant sponsor: National Science Foundation; contract grant number: CRIF CHC-99746320

Contract grant sponsor: IBM.

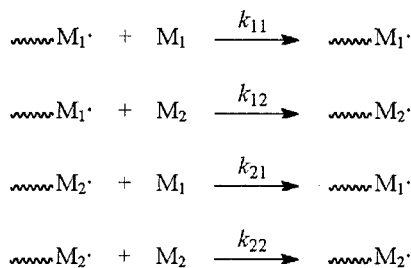


Figure 1 Terminal model of copolymerization.

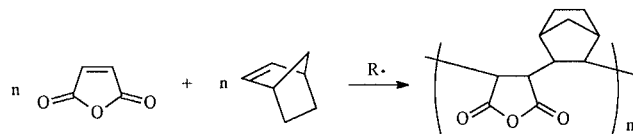
difficult to homopolymerize are often found to be capable of undergoing alternating copolymerization. For example, if a strong electron acceptor olefin is added together with a strong electron donor olefin, regular alternating copolymers may result from either a spontaneous initiation or a free-radical source.<sup>6</sup>

The mechanisms of most typical copolymerizations are typically between ideal copolymerization and alternating copolymerization. The mechanism of copolymerization becomes increasingly alternating as the  $r_1r_2$  product decreases from 1 toward 0. For polymerizations where the  $r_1r_2$  product lies somewhere between 0 and 1, the composition of the copolymer can be controlled to some extent by variation of the monomer feed ratio. However, as  $r_1r_2$  approaches very close to 0, the alternating behavior of the polymerization mechanism becomes the dominate factor and a 1 : 1 alternating copolymer is formed independent of the monomer feed ratio.

The terminal model also provides a useful means to approximate copolymer compositions that are dependent on such factors as the comonomer feed ratio and the reactivities of the comonomers according to the model. The Mayo–Lewis equation,<sup>7</sup> which is derived from the terminal model by using the assumption of the steady-state radical approximation, can be used to describe the instantaneous copolymer composition, as shown in Figure 2, where  $r_1$  and  $r_2$  are the respective monomer reactivity ratios.  $[M_1]$  and  $[M_2]$  describe the initial concentrations in the comonomer feed. The instantaneous mole fractions of the two repeating units in the copolymer are then defined as  $d[M_1]/d[M_2]$ . The terminal model, therefore, allows one to predict the instantaneous copolymer composition for a given comonomer feed simply on the basis of the comonomer reactivity ratios. Although the terminal model relies on several assumptions and may not be the most reliable model to describe a copolymerization process,

$$\frac{d[M_1]}{d[M_2]} = \frac{[M_1](r_1[M_1] + [M_2])}{[M_2]([M_1] + r_2[M_2])}$$

Figure 2 Mayo–Lewis copolymer composition equation.



Scheme 1 Radical alternating copolymerization of maleic anhydride and norbornene.

it is has the advantages of being simple to apply and very useful as a starting point to study a given copolymerization reaction.

Maleic anhydride (MAH) is the most widely studied comonomer for producing alternating copolymers. MAH contains very strong electron acceptin carbonyls and has been shown to homopolymerize poorly,<sup>8</sup> but will react with a number of electron-donating monomers to form alternating copolymers.<sup>9</sup> Of particular interest are many 1,2-disubstituted and cyclic olefins such as norbornene, that do not homopolymerize by free-radical methods, but will form alternating copolymers with maleic anhydride. Recently, main-chain alicyclic macromolecules produced from the alternating free-radical copolymerization of MAH with norbornene and norbornene derivatives have received attention as photoresist materials for 193-nm lithography.<sup>10</sup> Cyclic olefins such as norbornene will not homopolymerize to appreciable amounts via free-radical methods. However, when cyclic olefins are reacted with maleic anhydride, which is a strong electron acceptor, in the presence of a free-radical initiator, copolymerization occurs in an alternating manner (Scheme 1). In addition, maleic anhydride also serves to incorporate oxygen into the material, providing necessary adhesion and solubility properties that are required for imaging performance while still retaining sufficient etch resistance to be successfully demonstrated as 193-nm resist materials.<sup>11</sup> The cyclic olefin character of these materials provides for excellent etch resistance, surpassing even currently utilized phenol-based resists. Furthermore, the increased etch resistance is of great importance because of the decreasing film thickness necessary for the achievement of increasingly smaller feature sizes. In addition, the ability to modify polymer properties via incorporation of cyclic olefin monomer derivatives has further made this a very attractive route to new materials for 193-nm lithography.

Polymerization reaction data are traditionally obtained by careful sampling techniques followed by gravimetric and molecular weight analysis. Alternatively, samples can be withdrawn from the reactor and analyzed for residual monomer in solution at various times by chromatographic or spectroscopic techniques. Sample removal- techniques can be very difficult, especially because many reactions are extremely

sensitive to oxygen and other impurities that can be introduced during sampling. *In situ* mid-infrared spectroscopy is a desirable alternative, state-of-the-art, real-time, monitoring technique that is well suited to obtain real-time monomer conversion data for polymerization processes. In addition, reactions can be analyzed without complicated reactor modifications or expensive deuterated monomers. Previously, Long et al. utilized *in situ* near-infrared (NIR) (10,000–4000  $\text{cm}^{-1}$ ) spectroscopy by using fiber-optic probe technology to obtain solution polymerization kinetics of living anionic processes.<sup>12</sup> More recently, Puskas et al.<sup>13</sup> and Storey et al.<sup>4</sup> reported the application of *in situ* mid-infrared (4000–650  $\text{cm}^{-1}$ ) spectroscopy to monitor living cationic polymerization processes. In addition, Bradley and Long also applied *in situ* mid-infrared spectroscopy to study melt-phase acidolysis and ester exchange polymerization mechanisms.<sup>15</sup> Recently, McGrath and Wiles used *in situ* mid-IR spectroscopy to measure monomer conversion to determine the reactivity ratios for acrylonitrile/methyl acrylate radical copolymerization<sup>16</sup> via nonlinear methodologies first developed by Tidwell and Mortimer.<sup>17</sup> These previous efforts have demonstrated the utility of *in situ* infrared spectroscopy to obtain real-time structural and kinetic information for polymerization processes.<sup>18–20</sup> Herein, the use of *in situ* FTIR spectroscopy to measure reactivity ratios for norbornene/MAH radical copolymerization by using the well accepted Mayo–Lewis graphical method will be described.

## EXPERIMENTAL

### Materials

Norbornene (Nb) was purchased from Aldrich and vacuum distilled (0.1 mmHg) at room temperature from calcium hydride after degassing three times by using the traditional freeze–thaw method. After distillation, Nb was stored under positive nitrogen pressure as a solution in tetrahydrofuran (THF). MAH was purchased from Aldrich and purified via sublimation immediately prior to use. THF was distilled by using the classic sodium/benzophenone ketyl. All other reagents were purchased from Aldrich and used as received.

### Molecular weight characterization

Molecular weights were measured by using a Wyatt miniDAWN multiangle laser light scattering (MALLS) detector with a 690-nm laser (Wyatt Technology, Santa Barbara, CA) connected to a Waters SEC (515 pump, 717 autosampler, and 410 refractive index detector). The miniDAWN was connected in series after three

5- $\mu\text{m}$  Plgel mixed-bed columns (Polymer Laboratories, Amherst, MA). Measurements were made at 40°C with THF as the solvent at a flow rate of 1.0 mL/min.

### *In situ* mid-FTIR

*In situ* FTIR spectra were collected with a ReactIR 1000 (MCT detector, S/N = 7500, resolution = 4  $\text{cm}^{-1}$ ; ASI Applied Systems, Millersville, MD, www.asirxn.com) reaction analysis system equipped with a light conduit and DiComp (diamond-composite) insertion probe. Reaction data were analyzed by using ASI ReactIR software. The details and capabilities of the ReactIR 1000 reaction analysis system based on attenuated total reflectance (ATR) have been described in detail previously.<sup>21</sup>

### Example procedure with *in situ* FTIR for a maleic anhydride/norbornene copolymerization

In a 100-mL, round-bottomed, three-necked flask that was fitted with the ASI ReactIR 1000 DiComp probe was added a magnetic stir bar, Nb (9.40 g, 100 mmol), MAH (9.80 g, 100 mmol), and THF (14.4 mL). A schematic of the copolymerization reactor with *in situ* FTIR is illustrated in Figure 3. An oil bath at 65°C was raised until the reaction solution was completely immersed in the oil at 65°C. Once the temperature of the reaction mixture reached 65°C, 2,2-azobisisobutyronitrile (AIBN; 0.984 g, 6.00 mmol) was added to the flask. The flask was immediately purged with nitrogen for approximately 30 s and sealed tightly under positive nitrogen pressure (4–5 psi) with a rubber septum. The ReactIR was programmed to collect an FTIR spectrum of the reaction mixture every minute (64 scans) for the first hour of reaction and then every 5 min (256 scans) for the remainder of the reaction (FTIR data up to approximately 5–10% conversion was used for measuring the reactivity ratios). The reaction was then stirred at 65°C for 24 h while collecting FTIR spectra. After 24 h, the oil bath was removed and the reaction contents were allowed to cool to room temperature. After 24 h, the reaction mixture had solidified and was no longer stirred. The DiComp probe was removed from the reaction flask and THF (~ 50 mL) was added to dissolve the solid. The dissolved polymer was then precipitated into hexanes (~ 500 mL), filtered, and dried overnight under vacuum (0.1 mmHg) at ~ 75°C.

## RESULTS AND DISCUSSION

*In situ* FTIR was used to instantaneously monitor monomer conversion data in real time for the determination of reactivity ratios for Nb/MAH free-radical copolymerization (Scheme 1). A reaction flask was

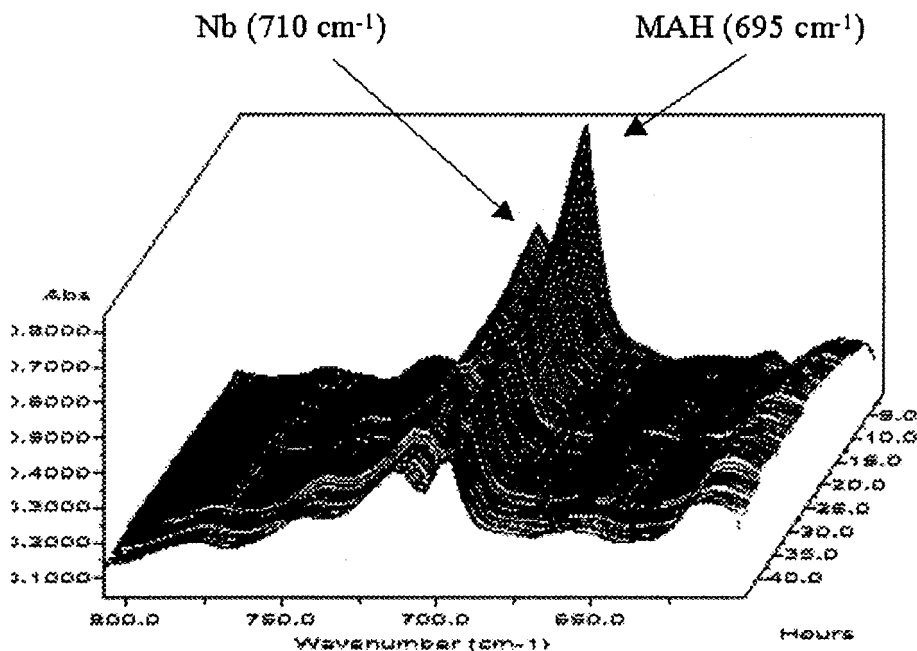
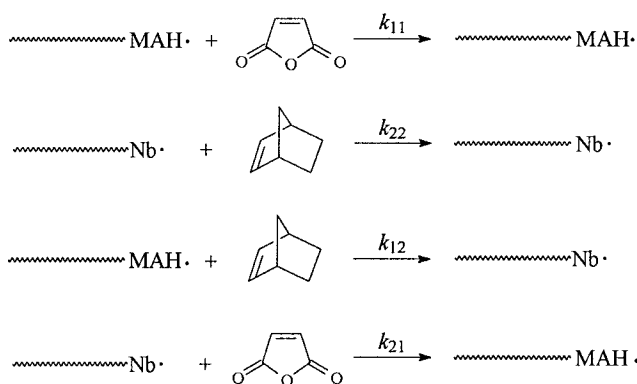


Figure 3 Vinylene region of waterfall plot of 50/50 Nb/MAH.

specifically designed to permit the introduction of the ATR-based infrared probe and attention was devoted to ensure the reactor was sealed to eliminate any volatilization of reaction components. Strong vinylene carbon-hydrogen ( $=C-H$ ) absorbances of the monomers were observed and allowed for kinetic analysis of the terpolymerizations by using *in situ* FTIR. The waterfall plot of the vinylene region for a Nb/MAH

(50/50 mol ratio) is illustrated in Figure 3. The vinylene carbon-hydrogen absorbance of Nb was observed at  $710\text{ cm}^{-1}$  and vinylene carbon-hydrogen absorbance of MAH was observed at  $695\text{ cm}^{-1}$ .

Pseudo-first-order kinetic plots were constructed from the data obtained via the *in situ* monitoring of the monomer absorbances. Initial kinetic interpretations focused on the assumption of pseudo-first-order kinet-



assuming negligible homopolymerizations of MAH and Nb,  $k_{11}=k_{22}=0$ , overall rate is:

$$\text{rate} = k_{12}[\text{MAH}\cdot](\text{Nb}) + k_{21}[\text{Nb}\cdot](\text{MAH})$$

assuming a steady state concentration of radicals and alternating copolymerization, rate is:

$$\text{rate} = (k_{12} + k_{21})[P\cdot][M]$$

where  $[P\cdot]$  = concentration of growing polymer radicals and  $[M]$  = concentration of MAH or Nb monomer and therefore an observed rate constant ( $k_{obs}$ ) is obtained from a plot of  $\ln[M]$  vs. time

$$k_{obs} = (k_{12} + k_{21})[P\cdot]$$

Figure 4 Pseudo-first-order alternating kinetic assumptions for a norbornene/maleic anhydride alternating copolymerization.

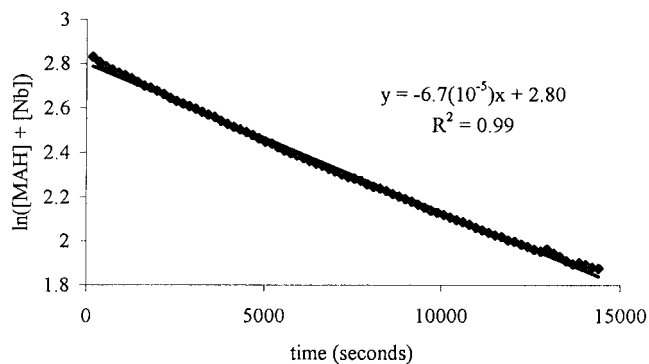


**Figure 5** Pseudo-first-order kinetic treatment of Nb and MAH concentration determined via *in situ* FTIR absorbances ( $670\text{--}725\text{ cm}^{-1}$ )

ics for an alternating polymerization mechanism (Fig. 4). Excellent agreement was observed by using these assumptions and linear kinetic plots were observed. A representative pseudo-first-order kinetic plot for a Nb/MAH copolymerization constructed from a plot of  $\ln[\text{monomer absorbance (total area from } 670\text{ to } 725\text{ cm}^{-1})]$  versus time (50/50 mol ratio,  $65^\circ\text{C}$   $k_{\text{obs}} = 6.7 \times 10^{-5}\text{ s}^{-1}$ ) is shown in Figure 5. As was expected for an alternating copolymerization mechanism, the fastest rate of copolymerization was observed for the 50/50 comonomer feed ratio (Table I).

Free-radical reactivity ratios of Nb and MAH were evaluated via graphical linear analysis of the rearranged copolymer composition equation (Fig. 6) based upon the terminal model developed by Mayo and Lewis.<sup>22</sup>

The graphical linear analysis method relies on measuring the copolymer composition to low degrees of conversion, such that a considerable change in the comonomer feed ratio does not occur. *In situ* mid-infrared spectroscopy was used to collect monomer concentration data to low degrees of conversion ( $\sim 10\%$ ) in real-time during free-radical copolymerizations of Nb and MAH. Monomer conversion data collected by using *in situ* FTIR were subsequently used to calculate the instantaneous copolymer composition ( $d[\text{MAH}]/d[\text{Nb}]$ ), which was calculated according to the terminal model. Infrared absorbances that were due to the olefinic functionality, which decrease as the monomers propagate, were identified for both Nb and MAH. Five different MAH/Nb comonomer feed compositions were analyzed, as follows: 40/60, 45/55, 50/50, 55/45, and 60/40.  $d[\text{MAH}]/d[\text{Nb}]$  values were

$$r_2 = \frac{[M_1]}{[M_2]} \left[ \frac{d[M_2]}{d[M_1]} \left( 1 + \frac{r_1[M_1]}{[M_2]} \right) - 1 \right]$$

**Figure 6** Rearranged copolymer composition equation.

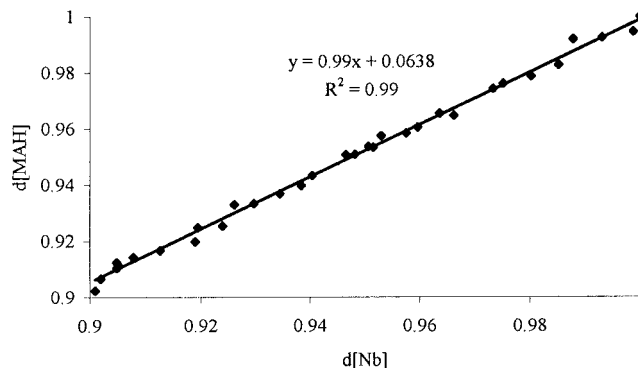


**Figure 7** Plot of  $d[\text{MAH}]$  versus  $d[\text{Nb}]$  for a 50/50 (mol ratio) MAH/Nb free-radical copolymerization measured using *in situ* FTIR.

obtained from plots of the monomer FTIR absorbance peak heights (Fig. 3), which were multiplied by the corresponding mole fraction in the starting comonomer feed. A representative  $d[\text{MAH}]/d[\text{Nb}]$  plot for the 50/50 MAH/Nb feed composition calculated to 10% conversion is shown in Figure 7. The  $d[\text{MAH}]/d[\text{Nb}]$  values for all five comonomer feed ratios are summarized in Table II. As discussed earlier, the theoretical value of  $d[M_1]/d[M_2]$  in the case of a perfectly alternating copolymerization mechanism, where  $r_{11}$  and  $r_{22}$  are equal to 0, is expected to be 1 regardless of the starting comonomer feed. As expected, the experimentally measured  $d[\text{MAH}]/d[\text{Nb}]$  values listed in Table II for all five different starting concentrations are approximately 1 within the experimental error of the method. The values randomly ranged from a low of 0.96 for the 40/60 [MAH]/[Nb] comonomer feed to a high of 1.0 for the 45/55 [MAH]/[Nb] comonomer feed.

The  $r_{\text{MAH}}$  and  $r_{\text{Nb}}$  values for each of the starting comonomer feed ratios were determined. Values for one of the reactivity ratios were assumed, and the value for the other reactivity ratio was calculated from the rearranged copolymer composition equation by using the known starting comonomer concentrations and the measured  $d[\text{MAH}]/d[\text{Nb}]$  values were measured by using *in situ* FTIR. For example,  $r_{\text{MAH}}$  and

**TABLE I**  
Observed Rate Constants MAH/Nb Copolymerizations as a Function of Starting Comonomer Feed

[MAH]/[Nb]	$k_{\text{obs}} (\times 10^5\text{ s}^{-1})^a$
40/60	3.9
45/55	5.7
50/50	6.7
55/45	6.3
60/40	5.4

<sup>a</sup> Determined via *in situ* FTIR up to 10% conversion.

**TABLE II**  
Comonomer Incorporation as a Function of Starting Comonomer Feed

[MAH]/[Nb] <sup>a</sup>	d[MAH]/d[Nb] <sup>b</sup>
40/60	0.96
45/55	1.0
50/50	0.99
55/45	1.0
60/40	0.99

<sup>a</sup> Starting comonomer feed ratio.

<sup>b</sup> Mole fractions incorporated into copolymer (determined via *in situ* FTIR) after approximately 10% conversion.

$r_{Nb}$  values for the 50/50 comonomer feed copolymerization are listed in Table III. Values ranging from  $-1.0$  to  $1.0$  were chosen for  $r_{MAH}$ , and  $r_{Nb}$  values were then calculated for each of the assumed  $r_{MAH}$  values. This process was repeated for all of the copolymerizations at different comonomer feeds. An estimation of the reactivity ratios by using the terminal model graphical method was then performed by means of graphing  $r_{MAH}$  versus  $r_{Nb}$  for all starting concentrations (Fig. 8). The average intersection points of the multiple plotted lines were then taken to be the estimated monomer reactivity ratios ( $r_{MAH} = 0.02$ ,  $r_{Nb} = 0.01$ ) with an error less than 10%.

## CONCLUSION

Free-radical reactivity ratios of Nb and MAH were evaluated via graphical linear analysis of the rearranged copolymer composition equation based upon the terminal model developed by Mayo and Lewis. Copolymerization data were collected via *in situ* FTIR to low degrees of conversion (approximately 10%) for copolymerizations of MAH and Nb. Copolymer composition data for 40/60, 45/55, 50/50, 55/45, and

**TABLE III**  
Example Calculated  $r_{Nb}$  Values Determined from the Rearranged Copolymer Composition Equation and Assumed  $r_{MAH}$  Values for a 50/50 MAH/Nb Copolymerization

$r_{MAH}$ (assumed)	$r_{Nb}$
-1	-1.00
-0.8	-0.79
-0.6	-0.57
-0.4	-0.36
-0.2	-0.14
0	0.07
0.2	0.28
0.4	0.5
0.6	0.71
0.8	0.93
1	1.14

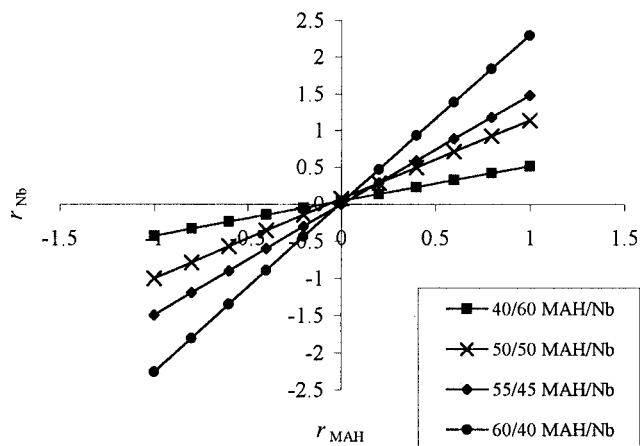


**Figure 8** Mayo-Lewis linear graphical analysis of MAH and Nb reactivity ratios.

60/40 MAH/Nb comonomer feed compositions were measured. Conversion data measured with *in situ* FTIR were then employed in conjunction with the rearranged copolymer composition equation to estimate MAH and Nb reactivity ratios. Both of the reactivity ratios were determined by using this method to be approximately 0 ( $r_{MAH} = 0.02$ ,  $r_{Nb} = 0.01$ ), which was a further indication of an alternating copolymerization.

Financial support provided by the Jeffress Memorial Trust, Virginia Tech Department of Chemistry, National Science Foundation (CRIF CHE-9974632), and IBM is gratefully acknowledged. The authors also thank the Center of Adhesive and Sealant Science (CASS) at Virginia Tech and the Adhesive and Sealant Council (ASC) for financial support through an ASC Education Foundation Research Fellowship.

## References

- Dostal, H. *Monatsh Chem* 1936, 69, 424.
- Mayo, F. R.; Lewis, F. M. *J Am Chem Soc* 1944, 66, 1594; Alfrey, T., Jr.; Goldfinger, G. *J Chem Phys* 1944, 12, 115; Wall, F. T. *J Am Chem Soc* 1944, 66, 2050.
- Polymer Handbook*, 3rd ed.; Brandrup, J.; Immergut, E. H., Eds.; Wiley: New York, 1989; Chapter 2, p. 153.
- Alfrey, T., Jr.; Price, C. C. *J Polym Sci* 1947, 2, 101.
- Odian, G. *Principles of Polymerization*, 3rd ed.; Wiley: New York, 1991; Chapter 6.
- Cowie, J. M. G. in *Comprehensive Polymer Science*; Allen, G.; Bevington, J. C.; Eastmond, G. C.; Ledwith, A.; Russo, S.; Sigwalt, P., Eds.; Pergamon Press: Oxford, 1989; Vol. 4, Chapter 22.
- Mayo, F. R.; Lewis, F. M. *J Am Chem Soc* 1944, 66, 1594.
- For a general review of maleic anhydride homopolymerization, see Gaylord, N. G. *J Macromol Sci Rev Macromol Chem* 1975, 13, 235; Regel, W.; Schneider, C. *Makromol Chem* 1981, 182, 237.
- Walling, C.; Briggs, E. R.; Wolfstirn, K. B.; Mayo, F. R. *J Am Chem Soc* 1948, 70, 1537; Barb, W. G. *J Polym. Sci.* 1953, 11, 117; Seymour, R. B.; Garner, D. P. *Polymer* 1976, 17, 21; Block, H.; Cowd, M. A.; Walker, S. M. *Polymer* 1972, 13, 549; Gaylord, N. G.; Maiti, S.; Patnaik, B. K.; Takahashi, A. *J Macromol Sci Chem*

- 1972, A6, 1459; Gaylord, N. G.; Maiti, S. J. *Macromol Sci, Chem* 1972, A6, 1481; Fujimori, K. J. *Macromol. Sci., Chem.* 1975, A9, 495; Caze, C.; Loucheux, C. J. *Macromol Sci, Chem* 1975, A9, 29.
10. Allen, R. D.; Opitz, J.; Larson, C. E.; Wallow, T. I.; Hofer, D. C. *Microolithog World* 5 (Winter 1999).
  11. Houlihan, F. M.; Wallow, T. I.; Nalamasu, O.; Reichmanis, E. *Macromolecules* 1997, 30, 6517.
  12. Long, T. E.; Liu, H. Y.; Schell, D. M.; Teegarden, D. M.; Uerz, D. S. *Macromolecules* 1993, 26, 6237.
  13. Puskas, J. E.; Lanzendörfer, M. G.; Pattern, W. E. *Polym Bull* 1998, 40, 55; Puskas, J. E.; Lanzendörfer, M. G. *Macromolecules* 1998, 31, 8684.
  14. Storey, R. F.; Donnalley, A. B.; Maggio, T. L. *Macromolecules* 1998, 31, 1523.
  15. Bradley, J. R.; Long, T. E. *Polym Prepr* 1999, 40 (1), 564.
  16. Wiles, K. B. M.S. Thesis, Virginia Polytechnic Institute and State University, Blacksburg, VA, 2002; Wiles, K. B.; Bhanu, V. A.; Pasquale, A. J.; Long, T. E.; McGrath, J. E. *Polym Prepr (Am Chem Soc, Div Polym Chem)* 2001, 42 (2), 608.
  17. Tidwell, P. W.; Mortimer, G. A. *J Polym Sci, Part A: Polym Chem* 1965, 3, 369.
  18. Pasquale, A. J.; Long, T. E. *Macromolecules* 1999, 32, 7954–7957.
  19. Lizotte, J. R.; Erwin, B.; Colby, R. H.; Long, T. E. *J Polym Sci, Part A: Polym Chem* 2002, 40, 583–590.
  20. Williamson, D. T.; Elman, J. F.; Madison, P. H.; Pasquale, A. J.; Long, T. E. *Macromolecules* 2001, 34, 2108–2114.
  21. Storey, R. F.; Donnalley, A. B.; Maggio, T. L. *Macromolecules* 1998, 31, 1523.
  22. Mayo, F. R.; Lewis, F. M. *J Am Chem Soc* 1944, 66, 1594.